ACTA IMEKO
ISSN: 2221-870X
March 2025, Volume 14, Number 1, 1 - 6

GNSS-based subsidence monitoring of the Shurtan gas reservoir in Uzbekistan

Dilbarkhon Fazilova[1,2], Fayzulla Tukhtameshov[1,3], Maftuna Rakhimberdieva[1,3], Aziz Kazakov[1,2], Khasan Magdiev[1,4]

[1] *Ulugh Beg Astronomical Institute of Uzbekistan Academy of Sciences, 33 Astronomy Street, 100052 Tashkent, Republic of Uzbekistan*
[2] *Tashkent state technical university named after Islam Karimov, 2, University Street, 100095, Tashkent, Republic of Uzbekistan*
[3] *National University of Uzbekistan named after Mirzo Ulugbek, 4, University Street, 100174, Tashkent, Republic of Uzbekistan*
[4] *Cadaster agency under Economy and Financial Ministry of Republic Uzbekistan, Chilanzar district, block Chilanzar-C, Chapanata Street, 100097, Tashkent, Republic of Uzbekistan*

ABSTRACT
This study investigates the impact of gas extraction on soil subsidence at the Shurtan Mining Complex in southern Uzbekistan, utilizing GNSS data. The complex, situated in the Beshkent trough within the Amu Darya Basin, represents a significant hub for hydrocarbon reserves, including gas, and gas condensate. Results indicate a correlation between gas extraction intensity and soil subsidence, with significant settlement observed at specific points most affected by extraction activities. Notably, annual height changes range from -0.5 mm/year to -3.4 mm/year, demonstrating the pronounced impact of gas extraction on subsidence. Tectonic processes, particularly pronounced at the transition boundary from the Tien Shan orogeny to the plain territory (Turan Plate), exert even greater influence on the nature of subsidence. Interpolation techniques, specifically Spline interpolation, are employed to visualize the spatial distribution and dynamics of terrain deformation. Key conclusions emphasize the correlation between gas extraction intensity and soil subsidence, alongside the influence of tectonic processes on height changes. Given the strategic importance of the Shurtan Mining Complex for Uzbekistan's economy, these findings hold significant implications for sustainable resource management and future research endeavors. This GNSS-based investigation offers valuable insights for advancing the understanding of geodynamic processes and informing resource management strategies in similar geological contexts.

Section: RESEARCH PAPER

Keywords: GNSS; mining activities; monitoring; vertical movements; Shurtan gas reservoir

Citation: D. Fazilova, F. Tukhtameshov, M. Rakhimberdieva, A. Kazakov, Kh. Magdiev, GNSS-based subsidence monitoring of Shurtan's gas reservoir in Uzbekistan, Acta IMEKO, vol. 14 (2025) no. 1, pp. 1-6. DOI: 10.21014/actaimeko.v14i1.1866

Section Editor: Leonardo Iannucci, Politecnico di Torino, Italy

Received April 15, 2024; **In final form** February 17, 2025; **Published** March 2025

Funding: This work was supported by State Basic funding from the Academy of Sciences of the Republic of Uzbekistan.

Corresponding author: Dilbarkhon Fazilova, e-mail: dilbar@astrin.uz

1. INTRODUCTION

In the modern world, the role of Global Navigation Satellite System (GNSS) measurements is paramount in resource management, addressing various practical tasks such as enhancing accuracy and efficiency, improving coordinate systems, assessing seismicity, resolving geodetic tasks, and more [1]-[7]. The integration of GNSS technology, in particular, provides a unique opportunity to study the dynamic nature of mineral extraction processes, offering a comprehensive understanding of spatial complexities influencing gas fields, thereby highlighting its significance in monitoring extraction areas [8]-[10].

The Shurtan Mining Complex, strategically situated in southern Uzbekistan, stands as a pivotal hub for natural gas extraction within the country. It represents a significant component of the hydrocarbon reserves delineated in the Amu Darya Basin in Central Asia. The complex, located within the Beshkent trough, an area that remains relatively underexplored, offers promising prospects for exploration, particularly with regards to reef and composite traps. Shurtan's deposits encompass various types of hydrocarbon reservoirs, including gas, gas condensate, and oil. These reservoirs, particularly

prevalent in the largely unexplored Beshkent depression, often form as a result of tectonic processes such as folding and fracturing of rock formations. Over the decades, extensive deep drilling and geophysical surveys have been conducted in this region to investigate subsurface structures and identify potential oil and gas deposits. This ongoing activity plays a vital role in advancing the region's mining industry and enhancing our understanding of resource distribution.

The pursuit of efficient resource extraction necessitates a profound understanding of the intricate interplay between geospatial dynamics and mining operations. Recent studies, including analysis of vertical terrain changes using geological [11] and radar data [12], underscore the need for continuous monitoring of ground subsidence in this area. Over the past 6 years (from 2016 to 2022), the vertical settlement of the development area has amounted to -2.34 cm [12]. Research suggests a potential anthropogenic origin of seismic activity in the vicinity of the Shurtan gas field, where intensive geological surveys may trigger earthquakes with magnitudes exceeding 5, similar to those recorded in Western Uzbekistan in 1976 and 1984 [13]. With plans to expand these research efforts, it becomes critically important to examine the impact of resource extraction and groundwater depletion on surface terrain. Studies on vertical displacements using geodetic methods are of great significance for the development of the mining industry and require further investigation due to potential implications for the terrain and the risk of induced seismic events. Within the scope of our research, we conducted, for the first time in this area, measurements using GNSS (Global Navigation Satellite Systems) to assess ground subsidence, allowing for a more accurate evaluation of geological processes and the preparation of recommendations for engineering and construction works.

2. DATA AND METHOD

2.1. Tectonic setting

The Shurtan Mining Complex, strategically located in southern Uzbekistan, serves as a key centre for natural gas extraction within the country and is classified as part of the hydrocarbon reservoirs delineated by reservoirs in the Kopet Dagh-Amu Darya Basin (KDADB). The KDADB extends across the territory of Turkmenistan, northeastern Iran, Uzbekistan, and the northern part of Afghanistan [14].

Situated in the Beshkent trough, an area that remains relatively underexplored, reef and composite traps here emerge as promising exploration targets [14], [15] (Figure 1). Shurtan's deposits encompass various types of hydrocarbon reservoirs, including gas, gas condensate, and oil. The primary reservoirs in the Shurtan deposit consist of Upper Jurassic carbonates and Lower Cretaceous siliciclastic rocks, predominant in the Beshtent trough. Reef and composite traps, housing the majority of undiscovered resources, are prevalent in the largely unexplored Beshkent depression, with carbonate formations at depths of approximately 3.5 km [17]. Since the 1950s, intensive deep drilling and geophysical surveys have been conducted to study subsurface rock formations and explore potential oil and gas reserves. This activity significantly contributes to the region's mining industry, providing valuable insights into resource distribution. These reservoirs often form due to tectonic processes like folding and fracturing of rock formations [18]. The total number of boreholes in this area has reached approximately 200. Pressure exerted by the fluid extracted from the wells is regularly measured near each active well using a barometer. To

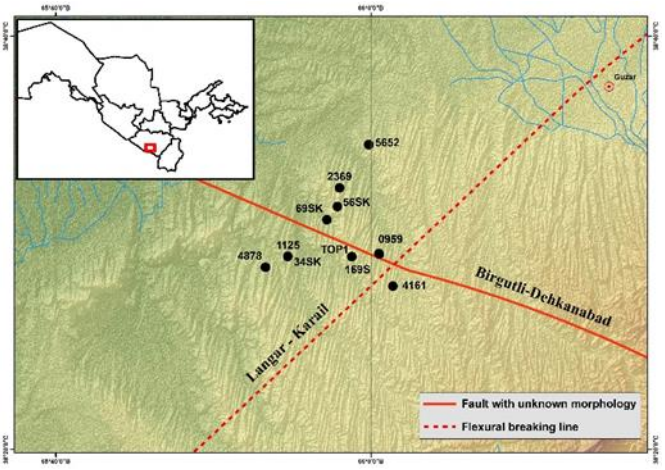

Figure 1. Study area and its location within the territory of Uzbekistan (small figure). Active faults (red lines) are compiled from [16].

assess the impact of this pressure on the study points, we calculated the average pressure values. These values were measured from 2 to 11 wells within a 1 km radius around each GNSS station. Next, a continuous surface was created using spline interpolation, which will be described in the 'Data and Methods' section (Figure 2). As shown in the figure, the main work has been concentrated in the central and eastern parts of the study area. This concentrated effort aims to further understand the geological structure and potential resource prospects in the region, facilitating future development and exploitation of hydrocarbon reserves.

2.2. GNSS data processing

This study represents the first investigation in this region, with previous measurements relying solely on levelling techniques. Utilizing levelling survey points, we carefully selected the station installation sites. To examine vertical movements, five cyclic measurements were conducted using GNSS at 11 points between 2022 and 2024, as depicted in Figure 1. The observations were conducted in static mode across a total of 5 sessions over a period of 2 years, with each session lasting from 3 to 4 days. The first observation stage took place on May 11-12, 2022. The second stage was conducted on July 14-17, 2022. The third stage occurred on October 21-23, 2022. The fourth observation stage was carried out on December 5-6, 2022. The fifth stage took

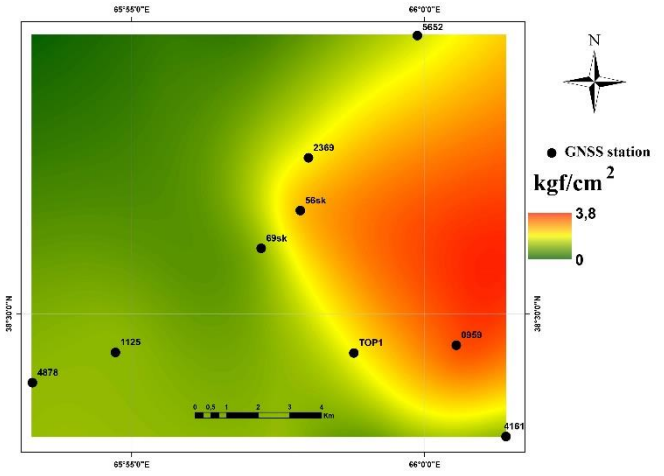

Figure 2. Map of the average pressure (kilogram-force per square centimetre, kgf/cm²), in wells around GNSS points in the Shurtan gas field.

place on March 27-30, 2023. The final stage was conducted on April 6-7, 2024. During the first year (2022), daily session durations were 12 hours, while during the second (2023) and third (2024) years, measurements were conducted continuously for 2-3 days. Observations were made using the SOUTH G1PLUS receiver with a built-in STHG1SG1Z-K508A antenna model. To minimize errors, the antenna elevation angle was set at 10 degrees, and data were collected at a sampling rate of approximately 30 seconds.

GPS only observation data were processed using the GAMIT/GLOBK v.10.71 software package [19], which included three stages [20]. *In the first stage*, daily phase measurements were used to estimate station coordinates and zenith atmospheric delay at each station, as well as satellite orbit parameters and Earth's orientation. Automatic iteration in the GAMIT block, utilizing the least squares method, is performed until the residuals between a-priori and estimated coordinates reach millimetre-level accuracy. During this process, cycle slips are either repaired or removed using double or triple differences of observations. High-precision geocentric orbits of IGS satellites were used for all solutions. Wide-lane ambiguities for each satellite were resolved at the 95% level using the Melbourne-Wubbena combination [21] and satellite code bias data. Additionally, standard models were chosen for the analysis: the IERS-1992 gravitational field model [22], a non-gravitational acceleration model for satellites [23], the Saastamoinen model for estimating dry and wet atmospheric delays [24], the GPT2 global pressure and temperature model [25] for zenith delay correction, and the FES2004 ocean tidal loading model [26]. To exclude the estimation of the orbital parameters and fix the IGS orbits, the processing was carried out in the baseline mode. The number of reference points and the session length affect the accuracy of the vertical component. According to the GAMIT developers' recommendations, the accuracy of the vertical component is estimated as follows: for a 1-hour session with 16 points, the accuracy is approximately 12 mm, while for a 12-hour session, it improves to around 4 mm. In order to link the regional measurements with the external global reference frame, the data from 16 continuously operating global tracking stations (ARTU, BADG, BHR4, CHUM, GUAO, HYDE, ISBA, IISC, KIT3, KRTV, MDVJ, NOVM, POL2, TASH, TEHN, URUM) were introduced in the processing. These data are mainly from the IGS permanent network.

In the second stage, daily files were combined into loosely constrained solutions for each session of the regional campaign. To achieve this, the solution files from the primary observations were converted into binary h-files. Then, to strengthen the reference frame for survey-mode observations, data from individual sessions (each lasting 3-4 days) were combined to obtain the averaged station coordinates for the multi-day experiment. Finally, *in the third stage*, the individual solutions were processed using the Kalman filter in GLOBK [27] to obtain a consistent set of station coordinates and velocities in the International Terrestrial Reference Frame ITRF2014 [28]. The reference frame was established using approximately 252 IGS stations from the IGb14 Core Reference Frame, with h-files derived from the global network and processed by Massachusetts Institute of Technology (MIT).

The processing in the program provides three primary levels of quality control for the initial data and the resulting coordinate solution. Firstly, for counting the expected data included, the number of x-files received was checked by the amount of initial RINEX files. Then the quality of the source data was assessed by the one-sided standard (RMS) deviations values for each satellite and station. For the network stations, the error range of the best points is from 4 mm to 6 mm, and that of the worst stations is from 9 mm to 13 mm. According to the program developers, values over 10 mm are high, but this is an acceptable noise level of external sources (such as bad quality of observation, multipath) [19]. Some of the new observation points have been reprocessed to refine the resulting coordinates. Finally, two criteria were used to check the validity of the solution. The baseline uncertainty values indicate the adequacy of the initial data for obtaining a reliable solution. Ambiguities were resolved with 89 % for the wide lane and 82 % for the narrow lane. These percentages suggest that the data quality and processing strategy are generally good, but the narrow-lane ambiguity resolution could be improved, possibly by increasing session length, refining the processing settings, or using additional constraints. The normalized RMS (square root of χ^2 per degree of freedom for the constrained solution with ambiguities free, constrained solution with ambiguities resolved, loose solution with ambiguities free, and loose solution with ambiguities resolved) is about 0.18-0.20 mm for all sessions. This value confirmed the conformity of the models to their noise level. The definitive check of the data and processing is provided by the time-series solution. The calculated solutions had a vertical coordinate uncertainty and repeatability, with the level of 2.9-8.3 mm. This error could have been affected by the 12-hour session.

This meticulous processing methodology ensures the accuracy and reliability of the derived coordinates and velocities, facilitating robust analysis and interpretation of the GPS data.

2.3. Velocity interpolation

Interpolated results of vertical velocities are essential for understanding the spatial distribution and dynamics of terrain deformation. By utilizing interpolation techniques, we can estimate height change velocities at unmeasured locations based on observations from surrounding points. These interpolated velocities provide valuable insights into the overall pattern of ground movement and can help identify areas of accelerated subsidence or uplift. Additionally, they serve as crucial inputs for predictive models and decision-making processes related to land use planning, infrastructure development, and environmental management. Thus, accurate and reliable interpolation of vertical velocities is paramount for comprehensive geodetic analyses and informed decision-making regarding land subsidence, uplift, and associated hazards. To obtain the velocity field for the region, the "Spline" interpolation method was used in the ArcGIS software ver.10.8 [27]. Spline interpolation is a mathematical technique that allows the creation of a continuous surface from a set of scattered points. This approach is useful when dealing with point data that is unevenly distributed across a study area and requires an estimate of the hazard distribution over the entire area. It involves fitting a smooth curve to a set of data points by minimizing the overall curvature of the curve. Several studies have utilized the Spline interpolation method for various applications, as documented in [29]-[32]. In our study, the regularized spline method was chosen for data interpolation, as it allows the creation of a smooth surface that passes precisely through the input points. The algorithm used for the Spline tool employs the following formula for surface interpolation [27]:

$$S(x,y) = T(x,y) + \sum_{j=1}^{N} \lambda_j R(r_j), \tag{1}$$

where j = 1, 2, … N, with N the number of points, λ_j - coefficients, obtained by solving a system of linear equations, r_j - the distance from point (x, y) to point j, and

$$T(x,y) = a_1 + a_2 x + a_3 y, \tag{2}$$

in which the a_i coefficients are obtained by solving a system of linear equations. Furthermore,

$$R(r_j) = \frac{1}{2\pi}\left\{\frac{r_j^2}{4}\left[\ln\left(\frac{r_j}{2\pi}\right) + c - 1\right] + \right. \\ \left. + \tau^2\left[K_0\left(\frac{r_j}{\tau}\right) + c + \ln\left(\frac{r_j}{2\pi}\right)\right]\right\}, \tag{3}$$

where τ^2 is a weight parameter equal to 0.001, K_0 – the modified Bessel function, and c is a constant equal to 0.577215.

The linear equations underlying this method are based on the following conditions: the surface must accurately fit the measured data and pass through all observation points, while also minimizing the overall curvature. This ensures that the interpolated surface faithfully represents the input data while smoothing variations to reduce total curvature.

The selection of this method is due to its ability to model gently varying surfaces, such as elevation, which is particularly important for our research. The regularized spline method also allows for controlling the smoothness of the surface using a weight parameter, which determines the influence of the third derivatives in the curvature minimization equation. In our case, the weight was set to 0.001, ensuring an optimal balance between surface smoothness and interpolation accuracy, avoiding excessive smoothing. The number of points used in the calculation of each interpolated cell was set to 9. This number allows for the influence of nearby points, creating a sufficiently smooth surface that fits the data without significantly increasing processing time.

Thus, the regularized spline method not only accurately reproduces the measured data but also minimizes curvature changes, making it ideal for tasks involving the interpolation of smooth surfaces.

3. RESULTS AND DISCUSSION

Annual changes in point elevation within the region are illustrated in Table 1. The table provides vertical (V_h) velocities, and their standard deviations (SDv_h) for each GNSS site. Figure 3 illustrates these changes graphically. The points (4161-112S), (0959-169S), (34SK-1125) are sites with two installations. The results are shown in the Table 1, and do not have significant differences, so they were not included in the Figure 3. The data reveal a prevalent trend of ground subsidence attributed to gas extraction activities. Primarily, the trend of intense subsidence is evident in the central part of the study area. Particularly noteworthy is the significant subsidence ranging from -2.4 mm/year to -3.4 mm/year observed at points 0959, TOP1, 2369, 56SK, and 69SK. This area has been the focus of extensive gas extraction efforts in recent years (see Figure 2). Moreover, the influence of regional tectonics should be acknowledged. The Langar-Karail flexure-fault zone separates the Tien Shan orogen from the Turan platform [33]. Situated in the transitional zone between the Tien Shan orogeny and the Turan Plate, the area may experience shifts from uplift zones to subsidence zones. The analysis of pressure data near the wells (Figure 2) and ground subsidence (Figure 3) reveals a correlation between these parameters, particularly in the central part of the field, where extensive gas extraction activities have been conducted in recent years. The central region shows the highest-pressure values and the most intense subsidence, confirming the impact of anthropogenic pressure on geodynamic processes. At station TOP1, the maximum subsidence of -3.4 mm/year is observed, which is attributed to both gas extraction and tectonic activity. Despite their proximity to station TOP1, stations 0959 and 4161 show a subsidence of -2.4 mm/year, possibly indicating the influence of orogenic activity.

Table 1. Vertical (V_h) velocities and their standard deviations (SDv_h) of each GNSS site. Duplicate points are marked with an asterisk (*).

Station	Longitude (°)	Latitude (°)	V_h (mm/yr)	SDv_h (mm/yr)
4161	66.023	38.465	-2.4	0.3
112S*	66.023	38.465	-2.4	0.3
0959	66.009	38.491	-2.6	0.2
169S*	66.008	38.491	-2.6	0.3
5652	65.998	38.579	-1.0	0.3
TOP1	65.979	38.489	-3.4	0.4
2369	65.967	38.544	-2.9	0.3
56SK	65.965	38.529	-3.9	0.8
69SK	65.954	38.519	-3.0	0.5
34SK*	65.912	38.489	-0.5	0.9
1125	65.912	38.489	-0.5	0.9
4878	65.888	38.480	-1.8	0.3

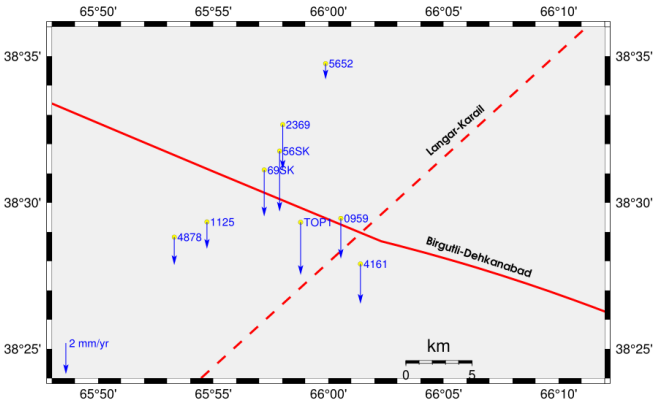

Figure 3. The annual height changes of the points. Red lines represent faults (designations are the same as in Figure 1).

To ensure continuous representation of the vertical velocity field in the study area, spline interpolation of the obtained values was performed (Figure 4). Spatial analysis confirms the trends in velocity changes caused by gas extraction, as well as reflects the geological structure of the region. However, despite confirming the overall trend, the interpolation results and the pressure data from the wells show slight discrepancies. This is likely due to the density of the measurement network and the number of stations in the study area, which may affect the accuracy and detail of the obtained data. Additionally, variations in local geological conditions, such as differences in soil composition or fault proximity, could also contribute to these observed deviations.

4. CONCLUSIONS

In this study, we conducted an analysis of vertical movements and height changes at the Shurtan deposit using GNSS data. Our findings lead to several key conclusions. Firstly, we found that the intensity of gas extraction correlates with the overall level of

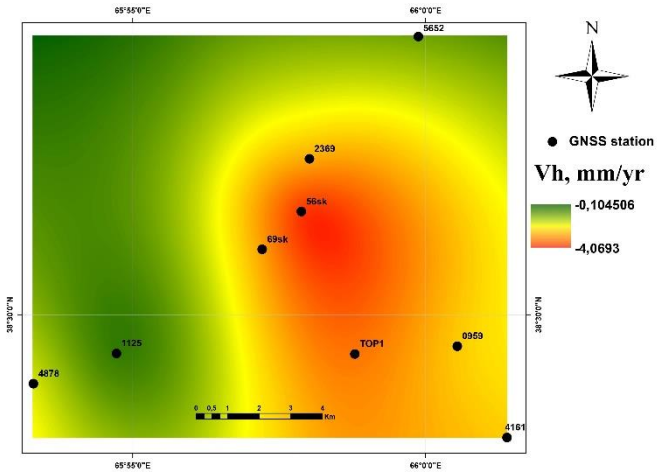

Figure 4. Surface generated based on Spline interpolation of elevation change rates.

soil subsidence, confirming the significant impact of this process on the geodynamics of the deposit. Particularly high settlement rates are observed at points located in the active gas extraction zone. Secondly, we emphasize the importance of tectonic processes affecting height changes at the deposit. Areas with pronounced tectonic activity exhibit significant height changes, indicating the influence of structural features on geodynamic processes. Additionally, our spline interpolation methodology allowed for a more visually informative representation of the results, highlighting areas with the most intense subsidence. Finally, our research underscores the importance of further monitoring of geodynamic processes at the Shurtan deposit and their impact on the safety and efficiency of gas extraction. Considering the complexity of the geological structure of the deposit and its strategic importance for the Uzbekistan economy, further studies in this area may have significant implications for the development of the mining industry and sustainable use of natural resources.

It is noteworthy that such GNSS-based investigations are conducted here for the first time, promising valuable insights for future research and resource management strategies. The accuracy of measurements is planned to be improved in the future by increasing the session durations and by processing data from other GNSS systems (GLONASS, Beidou, Galileo). Despite the current uncertainty in velocity, GPS measurements have proven to be reliable for monitoring the vertical movement dynamics in the region caused by gas extraction.

ACKNOWLEDGEMENT

GNSS data were processed using the GAMIT/GLOBK software. Some of the Figures were prepared using the GMT graphics package [34]. We would also like to thank reviewers for their many constructive comments and suggestions.

REFERENCES

[1] A. Angrisano, S. D. Pizzo, S. Gaglione, S. Troisi, M. Vultaggio, Using local redundancy to improve GNSS absolute positioning in harsh scenario, Acta IMEKO, 7 (2018) 2, pp. 16–23. DOI: 10.21014/acta_imeko.v7i2.538.

[2] M. Makhmudov, D. Fazilova, Construction the velocity field in a regular grid in the Tashkent region on the basis interpolation of GNSS permanent stations data, Proc. of the Int. conference InterCarto. InterGIS. GI support of sustainable development of territories, Moscow: MSU, Faculty of Geography, Russia, 2023, 29(1), pp. 535–545. [In Russian] DOI: 10.35595/2414-9179-2023-1-29-535-545

[3] H. T. Elshambaky, M. R. Kaloop, J. W. Hu, A novel three-direction datum transformation of geodetic coordinates for Egypt using artificial neural network approach, Arabian Journal of Geosciences, 11 (2018), DOI: 10.1007/s12517-018-3441-6

[4] D. Fazilova, O. Arabov, Vertical accuracy evaluation free access digital elevation models (DEMs): case Fergana Valley in Uzbekistan, Earth Sciences Research Journal, 27(2003), pp. 85–91. DOI: 10.15446/esrj.v27n2.103801

[5] G. Casula, M. G. Bianchi, Comparison of the historic seismicity and strain-rate pattern from a dense GPS-GNSS network solution in the Italian Peninsula, Geodesy and Geodynamics, 7(2016), pp. 303-316. DOI: 10.1016/j.geog.2016.06.003

[6] V. Baiocchi, S. D. Pizzo, F. Monti, G. Pugliano, M. Onori, U. Robustelli, S. Troisi, F. Vatore, F. J. L. Trujillo, Solutions and limitations of the geomatic survey of an archaeological site in hard to access areas with a latest generation smartphone: the example of the Intihuatana stone in Machu Picchu (Peru), Acta IMEKO, 11 (2022) 1, pp. 1–8. DOI: 10.21014/acta_imeko.v11i1.1117

[7] L. Alessandri, V. Baiocchi, F. Monti, L. Cusimano, A. Fiorillo, V. Gianni, C. Rossi, P. A. J. Attema, M. F. Rolfo, Low-cost GPS/GNSS RTK receiver to build a cartographic grid on the ground for an archaeological survey at Piscina Torta (Italy), Acta IMEKO, 12 (2023) 4, pp. 1–6. DOI: 10.21014/actaimeko.v12i4.1561

[8] Y. Cai, Y. Jin, Z. Wang, T. Chen, Y. Wang, W. Kong, W. Xiao, X. Li, X. Lian, H. Hu, A review of monitoring, calculation, and simulation methods for ground subsidence induced by coal mining, International Journal of Coal Science & Technology, 32 (2023), pp. 1–23. DOI: 10.1007/s40789-023-00595-4

[9] S. Zhang, J. Zhang, Ground Subsidence Monitoring in a Mining Area Based on Mountainous Time Function and EnKF Methods Using GPS Data, Remote Sensing, 14(2022), pp. 1–24. DOI: 10.3390/rs14246359

[10] D. Fazilova, M. Makhmudov, K. H. Magdiev, Analysis of Crustal Movements in the Angren-Almalyk Mining Industrial Area Using GNSS Data, International Journal of Geoinformatics., 19(2023), pp. 12–19. DOI: 10.52939/ijg.v19i11.2915

[11] A. Yarmukhamedov, Morphostructure of the middle Tien Shan and its connection with seismicity. Fan Tashkent, 1988, ISBN 5-684-00084, 166 pp. [In Russian] Online [Accessed 9 March 2025] https://www.geo-fund.am/files/library/1/15247392644395.pdf

[12] F. G‘. To‘xtameshov, A. B. Goipov, Application of radiolocation space imaging methods in surface movement monitoring of developing hydrocarbon deposits, Geology and Mineral Resources, 6 (2023), pp. 69-74. [In Uzbek] Online [Accessed 9 March 2025] https://api.scienceweb.uz/storage/publication_files/6785/17675/659b8fb006044___Number_6_2023%20(2).pdf

[13] B. Nurtaev, Earthquake hazard assessment in Uzbekistan: unanticipated impacts, Tashkent: Proc. of the Int. Conf. on Complexity in earthquake dynamics: From nonlinearity to earthquake prediction and seismic stability, 2012. pp.3-12.

[14] G. Hosseinyar, R. Moussavi-Harami, I. A. Fard, A. Mahboubi, Seismic geomorphology and stratigraphic trap analyses of the Lower Cretaceous siliciclastic reservoir in the Kopeh Dagh-Amu Darya Basin, Petroleum Science, 16(2019). pp. 776–793. DOI: 10.1007/s12182-019-0347-1

[15] Y. Yixin, Y. Jinyin, Z. Junzhang, L. Feng, T. Chongzhi, X. Xiaolong, W. Hang, Division and resources evaluation of hydrocarbon plays in the Amu Darya basin, central Asia. Petroleum exploration and development, 42(2015), pp. 821-826. DOI: 10.1016/S1876-3804(15)30078-1

[16] O. Tsay, Electronic map of faults of the Middle, Southern Tien Shan and adjacent territories, in Proc. of the LI Tectonic Meeting "Fundamental problems of tectonics and geodynamics", GEOS, Moscow, v.2(2019), pp.382-386. Online [Accessed 9 March 2025] http://www.ginras.ru/materials/files/MTS-2020-2%20.pdf
[17] G. F. Ulmishek, Petroleum geology and resources of the Amu-Darya Basin Turkmenistan Uzbekistan Afghanistan and Iran, U.S Geological Survey Publication, 2004, DOI: 10.3133/b2201H
[18] T. Sivaykova, Geological structure and prospects of oil and gas potentiality of the Bukhara-Jhiva region of Western Uzbekistan, Gubkin University Moscow, 2019, 166 pp. [In Russian] Online [Accessed 9 March 2025] https://www.dissercat.com/content/geologicheskoe-stroenie-i-perspektivy-neftegazonosnosti-bukharo-khivinskogo-regiona-zapadnog
[19] T. A. Herring, R. W. King, M. A. Floyd, S. C. McClusky, GAMIT reference manual. GPS Analysis at MIT, Release 10.7. Massachusetts Institute of Technology Cambridge, MA, USA, 2018, 168 pp. Online [Accessed 9 March 2025] https://geoweb.mit.edu/gg/docs/GAMIT_Ref.pdf
[20] D. Dong, T. A. Herring, R. W. King, Estimating regional deformation from a combination of space and terrestrial geodetic data, Journal of Geodesy, 72(1998), pp. 200–214. DOI: 10.1007/s001900050161
[21] M. Dubbini, P. Cianfarra, G. Casula, A. Capra, F. Salvini, Active tectonics in northern Victoria Land (Antarctica) inferred from the integration of GPS data and geologic setting, Journal of Geophysical Research, 115(2010), pp. 1–17. DOI: 10.1029/2009JB007123
[22] IERS Conventions 2010 (IERS Technical Note 36). G. Petit, B. Luzum (editors). Verlag des Bundesamts für Kartographie und Geodäsie, Frankfurt am Main, 2010, ISSN: 1019-4568, 179 pp. Online [Accessed 9 March 2025] https://iers-conventions.obspm.fr/content/tn36.pdf
[23] G. Beutler, E. Brockmann, W. Gurtner, U. Hugentobler, L. Mervart, M. Rothacher, Extended orbit modeling techniques at the CODE Processing Center of the International GPS Service for Geodynamics (IGS): theory and initial results, Manuscr. Geod. 19(1994), pp. 367–386. DOI: 10.1007/BF03655466
[24] J. Saastamoinen, Atmospheric Correction for the Troposphere and Stratosphere in Radio Ranging of Satellites, The Use of Artificial Satellites for Geodesy. Geophys. Monogr. 15(1972), pp. 247-251. DOI: 10.1029/GM015p0247
[25] K. Lagler, M. Schindelegger, J. Böhm, H. Krásná, T. Nilsson, GPT2: Empirical slant delay model for radio space geodetictechniques, Geophys. Res. Lett. 40 (2013), pp. 1069–1073. DOI: 10.1002/grl.50288
[26] F. Lyard, F. Lefevre, T. Letellier, O. Francis, Modelling the global ocean tides: modern insight from FES2004, Ocean Dynamics, 56(2006), pp. 394–415. DOI: 10.1007/s10236-006-0086-x
[27] T. A. Herring, M. A. Floyd, R. W. King, S. C. McClusky, GLOBK reference manual, Global Kalman filter VLBI and GPS analysis program, Release 10.6. Massachusetts Institute of Technology: Cambridge, MA, USA, 2015, 95 pp. Online [Accessed 9 March 2025] https://geoweb.mit.edu/gg/docs/GLOBK_Ref.pdf
[28] Z. Altamimi, P. Rebischung, L. Métivier, X. Collilieux, ITRF2014: A new release of the International Terrestrial Reference Frame modeling nonlinear station motions. Journal of Geophysical Research: Solid Earth, 121(2016), pp. 6109–6131. DOI: 10.1002/2016JB013098
[29] An overview of the Interpolation toolset. Online [Accessed 04 May 2023] https://pro.arcgis.com/ru/pro-app/3.0/tool-reference/spatial-analyst/how-spline-works.htm
[30] Q. Meng, Z. Liu, B. E. Borders, Assessment of regression kriging for spatial interpolation–comparisons of seven GIS interpolation methods, Cartography and geographic information science, 40(1) (2013), pp. 28-39. DOI: 10.1080/15230406.2013.762138
[31] A. Gharagozlou, A. Tayeba, M. Dadashi, H. Abdolahi, Zoning of CO Emissions in Tehran in the Medium Term by Using Third Quartile as the Exposure Candidate, Journal of Geographic Information System, 6 (2014), pp. 526-532. DOI: 10.4236/jgis.2014.65043.
[32] W. H. F. Smith, P. Wessel, Gridding with continuous curvature splines intension, Geophysics, 55 (3) (1990), pp. 293–305. DOI: 10.1190/1.1442837
[33] D. Atabaev, O. Mordvintsev, D. Mordvintsev, N. Atabaeva, Physical Properties of the Earth Crust Within the Joint Zone Between Turan Platform and Orogenic Structures of Tien-Shan, Earth Sciences. 8 (2) (2019), pp. 69-80. DOI: 10.11648/j.earth.20190802.11
[34] P. Wessel, J. F. Luis, L. Uieda, R. Scharroo, F. Wobbe, W. H. F. Smith, D. Tian, The Generic Mapping Tools Version 6, Geochemistry, Geophysics, Geosystems, 20(2019), pp. 5556–5564. DOI: 10.1029/2019GC008515